Chapter 29
Optimal Design and Techno-Economic Analysis of a Microgrid for Community Load Applications

Venkatesh Boddapati and S. Arul Daniel

Abstract The energy demand is increasing day by day, and fossil fuels are depleting; it is necessary to tap the untapped renewable energy to meet the increasing energy demand. For effective utilization of renewable energy, it is imperative to design and develop the community-level microgrids. Thus, this paper intends the optimal design of a community-level microgrid for available load at BMS College of Engineering, Bengaluru, India. The proposed microgrid consists of hybrid renewable energy sources, such as solar PV, wind turbine, battery storage, and diesel generator. To maintain the reliability of the power supply and to meet the peak load demand during the peak load hours, a diesel generator is proposed. The proposed microgrid is modeled, optimized, and simulated by using the hybrid optimization model for multiple energy resources (HOMER). The levelized cost of energy (LCOE), the net present cost (NPC), and operating cost (OC) are considered for the economic analysis and modeling of microgrid. In autonomous mode, the LCOE, NPC, and OC are estimated as 0.319 $/kWh (22.33 ₹/kWh), $4881,583 (₹341,710,810), and $12,519.34 (₹876,353.8) while in grid-connected mode, the LCOE, NPC, and OC are estimated as 0.0534 $/kWh (3.738 ₹/kWh), $128,621 (₹9,003,470), and $144.84(₹10,138.8), respectively. Further optimum size of the proposed microgrid is also presented. Furthermore, the obtained results are compared with existing models and found that the designed system is superior in terms of cost and sizing.

Keywords Microgrid · Hybrid energy systems · Optimization · Techno-economical analysis

V. Boddapati (✉) · S. A. Daniel
Department of Electrical and Electronics Engineering, National Institute of Technology, Tiruchirappalli, Tamil Nadu, India
e-mail: venkateshb.eee@bmsce.ac.in

S. A. Daniel
e-mail: daniel@nitt.edu

P. V. Baredar et al. (eds.), *Advances in Clean Energy Technologies*,
Springer Proceedings in Energy, https://doi.org/10.1007/978-981-16-0235-1_29

29.1 Introduction

As of May 2020, India is having 370,348 MW of power generation installed capacity; it includes power generation from different sources such as thermal, hydro, nuclear, and renewable energy sources. Fig. 29.1 indicates the percentage of power generation from various sources in India. The percentage of power generated from renewable sources is very less; the objective of the Ministry of New Renewable Energy (MNRE) is to install 175 GW of power generation from renewable energy sources by 2022. To meet the mission of the MNRE, it is necessary to develop the infrastructure required to tap the untapped non-conventional energy sources such as solar, wind, and biomass [1].

Hybrid energy generation received a significant advantage in recent years due to the advancement of renewable energy sources. The problems when designing the microgrids with the help of hybrid renewable energy sources are optimal design, power management, and reliability. The selected microgrid model must be optimized in terms of sizing and cost. Among all renewable energy sources, solar and wind sources have tremendous potential for community load electrification [2]. Many studies presented hybrid renewable energy system design for different load applications such a commercial load, community load, and industrial load applications. Hybrid energy systems consist of different combinations of renewable energy sources such as solar PV, wind, biomass, fuel cell, tidal, and hydel [3]. Most of the hybrid energy system models are designed for the autonomous microgrid application. The integration of renewable sources into the grid is an exciting job because of the unpredictable nature of renewable energy sources. The grid integration acts as a backup for the autonomous microgrid; the grid-connected system has certain advantages such as a grid-connected system which eliminates usage of battery and diesel generator.

One more model is designed in Ghana to check the feasibility of standalone hybrid energy system, and in that feasibility study, the LCOE and NPC of two systems are estimated as 0.382 $/kWh and $8,649,054 for the PV-wind-DG-battery system, while wind-DG-battery system records as 0.3926 $/kWh and $8,966,700 [4].

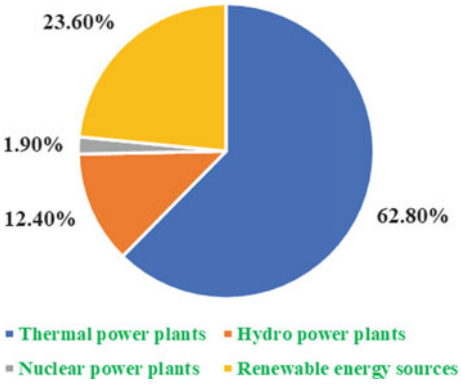

Fig. 29.1 Power generation from different sources

Many studies presented the techno-economical performance assessment of the grid-connected and an off-grid system with the help of different tools such as PVsyst, HOMER, and by using real-time data [5–10].

The objective of this work is the modeling of a microgrid for a community load available in BMS College of Engineering, Bengaluru. The proposed model is designed by using the HOMER simulator. The organization of the work carried is represented in the following steps.

- Modeling of microgrid with the help of HOMER simulation software.
- Finding the optimum sizing and least levelized cost of energy by reducing the annual cost of the total system.
- Performance analysis of the system during grid-integrated mode and autonomous mode of operation.
- Sensitivity analysis of the system by varying the inflation rate, discount rate, and fuel cost.

29.2 Methodology Used for the Analysis

29.2.1 Locations and Weather Conditions of the Selected Site

The selected site for the design is located on latitude 12° 56′ 19.01″ N and longitude 77° 33′ 34.19″ E, in Bengaluru, India. Selecting a proper location is very important for the HOMER simulation; the software has the option to select the proper location, and there is an option to select metrological data sources of the particular location [2]. In this study, the data selected for the analysis purpose is the National Aeronautics and Space Administration (NASA). As per the data received from the NASA, the average daily solar radiation changes from 4.5 to 6.5 kWh/m^2/day. The maximum radiation is found in March, and the lowest irradiation is found in July. The variation of irradiation is presented in Fig. 29.2, the variation of temperatures for the selected location is represented in Fig. 29.3, and the annual average wind speed measured by an anemometer height of 50 m is 2.82 m/s (Fig. 29.4).

Fig. 29.2 Solar irradiation variation and clearness index of the selected site

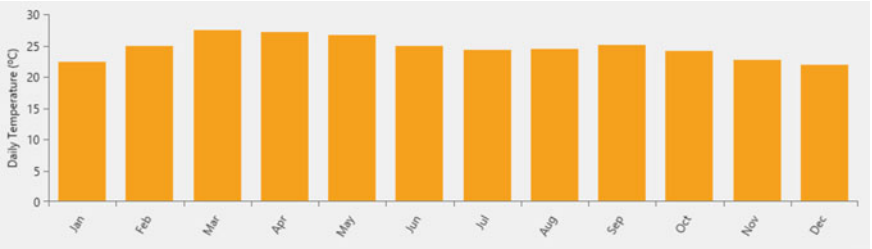

Fig. 29.3 Temperature variation of the location

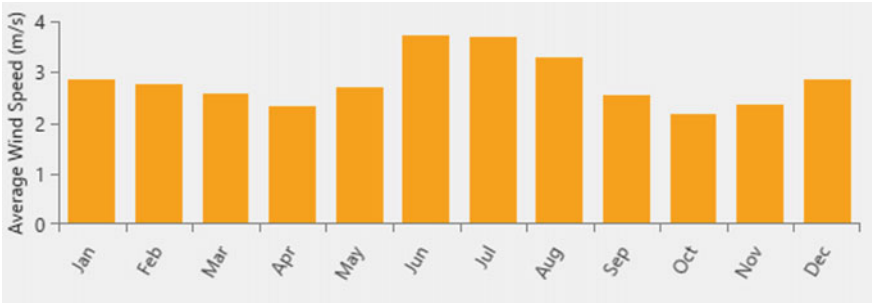

Fig. 29.4 Average wind variation

29.2.2 Schematic Diagram of the Proposed System

The proposed model is designed in two modes of operation, autonomous mode, and grid-connected mode. Figures 29.5 and 29.6 demonstrate the modeling of the proposed microgrid in the autonomous mode and grid-connected mode of operation. The proposed model consisted of a solar PV system, wind turbine, two diesel generators, and battery storage. Since the load is working with AC supply, it is necessary to convert the generated DC power into AC power, and the inverter is connected

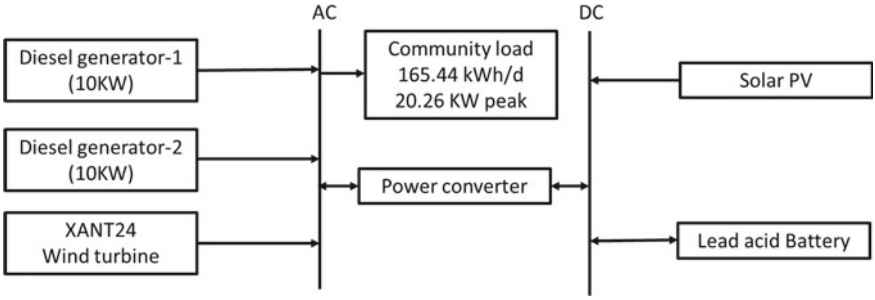

Fig. 29.5 Autonomous microgrid model

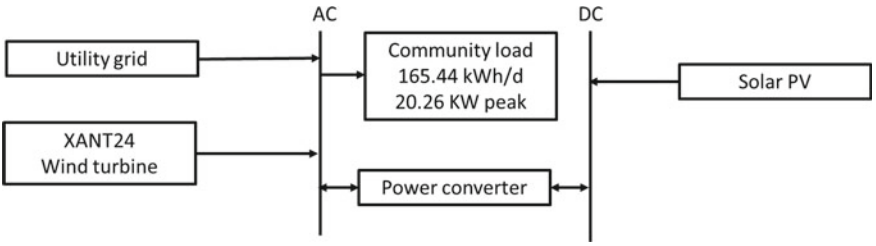

Fig. 29.6 Grid-connected microgrid model

between the solar PV and the AC loads. When the excess power is generated from the sources, there must be some storage equipment to store; the lead-acid battery is used for the storage purpose. All technical parameters and ratings of the system are represented in the schematic diagram of the autonomous microgrid.

29.2.3 Solar Array

The solar PV module consisting of the photovoltaic cell, which converts the radiation into electrical energy. The output power can be assessed based on the equations and module specifications given by the manufacturer. The output of the module depends upon the input irradiance and temperature; it is assumed that the output power is proportional to the input irradiance. The output power for the PV module can be calculated using Eq. (29.1)

$$P_{\mathrm{Sol}^{(t)}=P_{\mathrm{rat}}} f_{\mathrm{loss}} \frac{G_h}{G_s}\left[1+\alpha_p(T_C - T_s)\right] \tag{29.1}$$

P_{rat} represents the solar power output capacity of the solar PV panel, f_{loss} is represented as a loss of the solar panel; loss factor includes the losses due to partial shading, temperature, and drift. G_h indicates hourly solar incident radiation on solar panel (W/m^2). G_s indicates standard incident irradiation (1000 W/m^2), α_p is the temperature coefficient of the power, T_c is the current cell temperature in the current step, and T_s is the PV cell temperature under STC.

29.2.4 Wind Turbine

The power curve indicates the amount of power produced by the wind turbine as a function of wind at hub height. The output power of the wind turbines mainly depends upon the speed of the wind. The quadratic model can calculate the output power produced by the wind turbine by using Eq. (29.2), and for the study purpose,

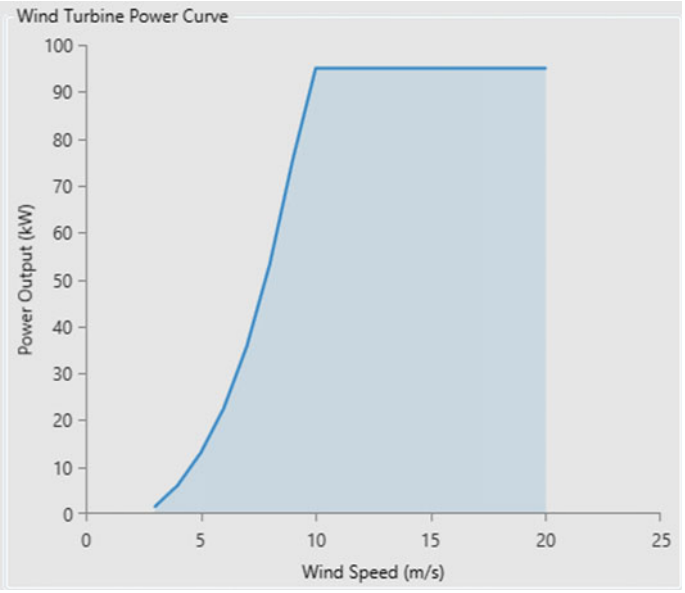

Fig. 29.7 Power curve for the XANT24 (95 KW) wind turbine

XANT24 (95 KW) wind turbine is used. The wind turbine power curve is represented in Fig. 29.7.

$$P_w(V_v) = \begin{cases} P_n \dfrac{v_v^2 - v_d^2}{v_n^2 - v_d^2}, & V_d < V_v < V_n \\ P_n, \ V_n \leq V_v < V_c 0, \ V_v \leq V_d \quad \text{and} \quad V_v \geq V_c \end{cases} \tag{29.2}$$

where P_w represents the output power produced by the wind turbine, P_n indicates the nominal power, V_d is the cut-in speed of the wind, V_c indicates cut off the speed of the wind, and V_n is the rated wind speed.

$$\frac{V(z)}{V(z_a)} = \left(\frac{z}{z_a}\right)^{\propto}. \tag{29.3}$$

To assess the power developed by the wind turbine, it is necessary to calculate the wind speed. The wind speed for specific high is calculated by using Eq. (29.3)

29.2.5 Power Inverter

The power generated by the solar PV panel is DC; since the load is working with AC supply, it is necessary to convert the generated DC power into AC power. The inverter is used for converting DC power into AC power with a constant frequency with inbuilt MPPT. The amount of power inverter that it can convert depends upon the rating of the inverter used.

$$P_{\text{inv}}(t) = P_{\text{pv}}(t)\eta_{\text{inv}} \tag{29.4}$$

where $P_{\text{pv}}(t)$ represents the total output power PV system and η_{inv} indicates inverter efficiency.

$$P_{\text{pv}}(t) = P_{\text{sol}}(t)N_{\text{sol}} \tag{29.5}$$

$P_{\text{sol}}(t)$ indicates the power generated from a single solar PV cell, and N_{sol} represents the number of solar PV panels. In an integrated grid system, the size of the inverter depends on two factors, such as grid sale capacity and local load demand.

$$P_{\text{max.inv}} = P_{\text{L.max}}(t) + P_{\text{gs.max}} \tag{29.6}$$

where $P_{\text{L.max}}(t)$ represents the maximum load demand and $P_{\text{gs.max}}$ indicates the maximum amount of power sold to the grid.

29.2.6 Utility Grid

The system is operated in two modes of operation, grid-connected mode and off-grid mode of operation. In the grid-integrated mode, if the power generated by the hybrid energy system is more than the load requirements that excess power generated is sent to the utility grid. The power supplied to the grid is calculated as

$$P_{\text{gs}}(t) = \left[P_{\text{pv}}(t)\eta_{\text{inv}} + P_{\text{w}}(V_{\text{v}})(t)\right] - P_{\text{L}}(t) \tag{29.7}$$

The power generated by the system is not sufficient, power is drawn from the grid, the amount of power drawn from the grid is calculated as

$$P_{\text{gp}}(t) = P_{\text{L}}(t) - \left[P_{\text{pv}}(t)\eta_{\text{inv}} + P_{\text{w}}(V_{\text{v}})(t)\right] \tag{29.8}$$

29.2.7 Diesel Generator

To improve the reliability of the off-grid system and to meet the sudden occurring of peak loads, the diesel generator is connected in the off-grid mode operation. The selected renewable sources such as wind and solar systems depend upon the climatic conditions, and the solar and wind are not reliable sources. In the off-grid system, power must be provided to consumers all the time, and there should not be any power cuts; to meet this objective, two 10 KW diesel generators are used. The fuel consumed by the diesel generator depends upon the output power requirement. The fuel consumed by the diesel generator is calculated as

$$F = F_0 Y_{\text{gen}} + F_1 P_{\text{gen}} \tag{29.9}$$

where F indicates fuel consumed in liters, F_0 indicates the generator fuel curve intercept coefficient (L/h/kW), and Y_{gen} is the rated capacity of the generator. F_1 fuel curve slope for the generator (L/h/kW) and P_{gen} indicate generator output in kW.

Where $v(z)$ represents the average wind speed at the new level z, v (z_{a}) indicates average wind speed at anemometer level z_a, and α represents power index.

29.3 Financial Matrices

This section aims to verify the economic feasibility of the model and find out the levelized cost of energy (LCOE). The LCOE is defined as the ratio of the sum of the entire cost collected during the project lifespan to the unit of electricity produced over the entire lifetime of the project. In this advanced analysis, the inflation and discount rates are considered as 2, 4, 6, 8, and 10%, and the effect of inflation and discount rates on the LCOE are also assessed.

$$\text{LCOE} = \left(\sum_{i=0}^{T}\left[\frac{C_i + L_i + O\&M + I_i}{(1+d)^i}\right]\right) / \left(\sum_{i=0}^{T}\left[\frac{E_i}{(1+d)^1}\right]\right) \tag{29.10}$$

where C_i represents the expenses form the cost of the system, L_i indicates the cost of the land, $O\&M_i$ is the entire operation and maintenance, I_i indicates insurance cost which is paid yearly during the project lifetime T, and d is the discount rate. Determined LCOE is useful for the investor to invest in hybrid energy system projects.

In this work, the opted system is based on the minimum total net present cost (NPC). The NPC (life cycle cost) is defined as the present value of the total cost of the system throughout the project lifetime, minus the present value of the total revenue that happened during the project lifetime. The NPC of each component of the system and overall cost of the system is calculated by using Eq. (29.11)

$$\text{NPC} = \frac{C_{\text{ann,tot}}}{\text{CRF}\left(i,\, R_{\text{proj}}\right)} \tag{29.11}$$

Here, $C_{\text{ann.tot}}$ indicates the total annualized cost; i is the total annual interest rate, CRF(i, N) is the capital recovery factor, which is calculated by Eq. (29.12) R_{proj} is the life of the project N represents the number of years.

$$\text{CRF}_{(i,N)} = i(1+i)^N / \left((1+i)^N - 1\right) \tag{29.12}$$

29.4 Result and Discussions

This section indicates the result analysis of autonomous and grid-connected microgrid. The simulator analyzes the system performance depending on the input data for 25 years. The HOMER considers the optimal system among available combinations. The system is operated in two modes operation, autonomous mode, and grid-connected mode. The hybrid energy system is optimized to meet the load demand. The effect of variation in inflation, diesel price, and the discount rate is also considered. The daily community load variation for the selected area is estimated at 165.44 kWh/day. Figure 29.7 demonstrates the instantaneous load variation of the selected community load.

29.4.1 Autonomous Mode of Operation

The obtained results for the LCOE, NPC, and OC for the autonomous microgrid system are 0.319 $/kWh (22.33 ₹/kWh), $4,881,583 (₹341,710,810), and $12,519.34 (₹876,353.8), respectively. The capital cost of the system is given in Table 29.1. In autonomous mode, the diesel generator is operated to meet the peak load demand and improve the reliability of the microgrid.

The electrical power production during the autonomous mode operation is demonstrated in Fig. 29.8. In the autonomous mode of operation, the solar PV system produces 45.6%, wind turbine produces 35.6%, diesel generator-1 produces 18.5%, and diesel generator-2 produces 0.350. Diesel generator-2 is kept as ideal, the contribution of the diesel generator is very less, but to improve the reliability of the system, the diesel-2 kept ideal for all most all the time.

The simple payback period of the autonomous microgrid is assessed as 4.72 years. The pay period obtained is very less; it gives a positive impression for the investors. This is a very less period to get back the investment. The seasonal load profile is represented in Fig. 29.9.

Table 29.1 Net present cost summary of the component

Component	Capital cost in $	Replacement	O&M ($)	Fuel cost in $	Salvage cost in $	Total ($)
Generator 10 KW-1	5000	7500	16,605	14,0362.9	1550	16,7917.9
Generator 10 KW-2	5000	7500	510	2971.48	4433.33	11,548.15
PV 25 KW	50,000	0	6250	0	0	56,250
Battery 1 kWh (112 numbers)	33,600	100,800	28,000	0	10,532.62	151,867.38
XNT M-24 (95 KW) Wind turbine	75,000	75,000	250	0	56,250	94,000
System	168,600	190,800	51,615	143,334.38	72,765.95	481,583.43

Fig. 29.8 Community load profile of the BMS College of Engineering

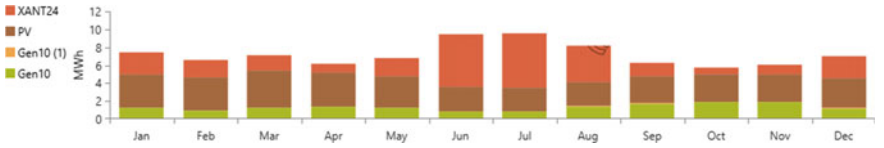

Fig. 29.9 Energy produced in autonomous mode

29.4.2 Grid-Connected Mode

The results found for the LCOE, NPC, and OC for the grid-connected system is 0.0534 $/kWh (3.738 ₹/kWh), $128,621 (₹9,003,470), and $144.84(₹10,138.8), respectively. The total cost of the system is estimated at $128,621.08. The electrical power production during the grid-connected mode operation is demonstrated in Fig. 29.10. In the grid-integrated mode of operation, the solar PV system produces 40.5%, wind turbine produces 31.6%, and the grid purchase is 27.9%. The energy produced by the renewable energy sources in each month and energy sold to the grid

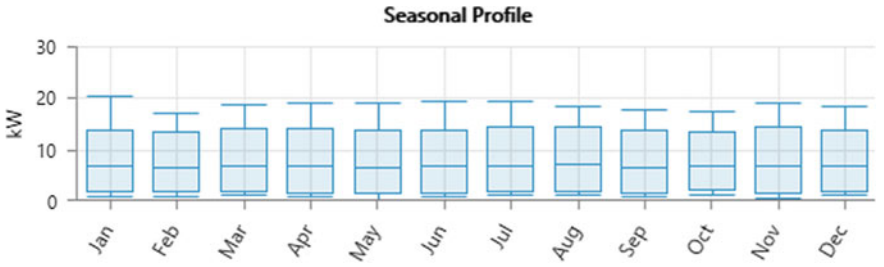

Fig. 29.10 Seasonal load profile

Table 29.2 Details of the energy purchased and energy sold to the grid in the grid-connected mode of operation

Month	Energy purchased (kWh)	Energy sold (kWh)	Net energy purchased (kWh)	Peak load (KW)	Energy charges in $
Jan.	2332	3328	−996	20	99.59
Feb.	1878	2944	−1066	16	106.59
Mar.	2348	2812	−464	17	46.44
Apr.	2495	2159	336	19	33.63
May	2233	2563	−330	19	33.02
Jun.	1612	5137	−3525	16	352.48
Jul.	1754	5249	−3494	19	349.45
Aug.	2262	3633	−1372	18	137.16
Sep.	2591	2058	533	18	53.28
Oct.	2730	1368	1368	17	36.79
Nov.	2720	1797	923	19	92.25
Dec.	2198	2762	−564	17	56.39
Annual	27,153	35,805	−8652	20	865.16

are given in Table 29.2. While doing the analysis, the energy purchased from the grid is considered as $0.1/kWh (₹7/kWh), and energy sold to the grid is considered as $0.15/kWh (₹10.5/kWh).

29.4.3 Sensitivity Analysis

The objective of the sensitivity analysis is to assess the sensitive parameters on the project. İn the sensitivity analysis, the variation of diesel price, inflation rate variation, and discount rates are considered. The diesel price variation is considered as 1 $/L (₹70/L), 1.5 $/L (₹105/L), and 2 $/L (₹140/L). The effect of LCOE and NPC is shown

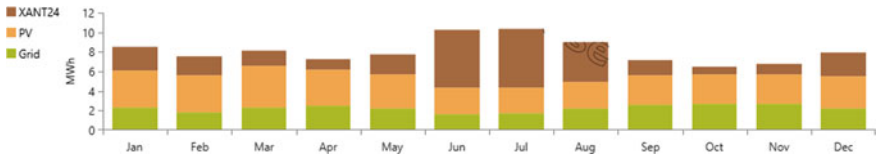

Fig. 29.11 Electricity production from the grid-connected mode

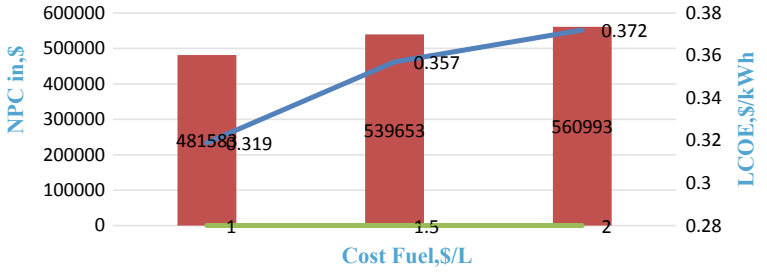

Fig. 29.12 Effect of diesel price on LCOE and NPC

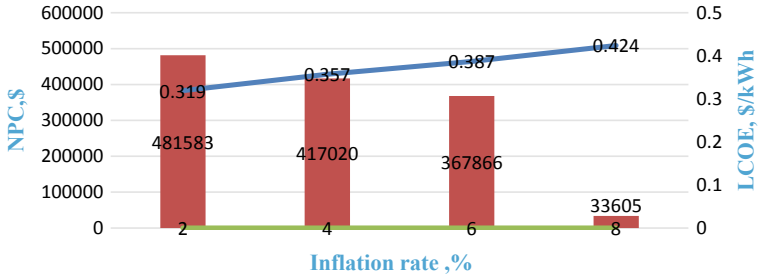

Fig. 29.13 Effect of inflation rates on LCOE

in Fig. 29.11. Similarly, the effect of inflation and discount rates is considered as 2, 4, 6, and 8%. The effect of LCOE and NPC demonstrated in Figs. 29.12 and 29.13

The effectiveness of inflation on the NPC is also essential; increasing the inflation rate decreases the NPC. The inflation rate is an essential parameter in the feasibility of the project (Fig. 29.14).

29.4.4 Optimum Sizing of the System

The optimum sizing of the components is given in Table 29.3.

Fig. 29.14 Effect of discount rates on LCOE

Table 29.3 Optimum sizing details of the components

Autonomous mode	Grid-connected mode
Diesel generator-1 (10 KW)	Utility grid
Diesel generator-2 (10 KW)	PV-25 KW
PV-25 KW	Converter 24–50 KW
1 kWh LA-112 numbers	(Wind turbine) XANT24-1
Converter 24–50 KW	–
(Wind turbine) XANT24-1	–

29.4.5 Future Scope

Microgrid design with hybrid energy systems is a growing area to meet the increasing global energy demand and optimum utilization of renewable energy sources possible with the help of hybrid energy system design. The hybrid renewable energy-based microgrid can be used for the electric vehicle charging station and rural electrification.

29.5 Conclusions

The objective of work aimed at the optimum modeling of a microgrid in terms of the sizing of the components and economic feasibility. The system is modeled by using hybrid energy sources such as solar, wind, and diesel generators. The proposed system is tested for the two modes of operations, and the optimum results are presented. The percentage of energy produced from each source to meet the load demand is presented. The designed model is compared with existing literature; it is found that the design is superior compared to other existing systems. The sensitivity analysis also carried out to see the effect of the performance of the system. The LCOE, NPC, and OC for an autonomous mode of operation are found as 0.319 $/kWh (22.33 ₹/kWh), $4,881,583 (₹341,710,810), and $12,519.34 (₹876,353.8). The LCOE, NPC, and OC for a grid-connected mode operation are calculated as 0.0534 $/kWh (3.738 ₹/kWh), $128,621 (₹9,003,470), and $144.84

(₹10,138.8). The optimum sizing of the distributed generator is also assessed. Form the analysis, and it is concluded that the grid-connected system is more economical than the autonomous mode operation.

References

1. Government of India, Ministry of Power. https://powermin.nic.in/
2. HOMER, https://www.homerenergy.com/products/pro/index.html
3. S. Singh, S.C. Kaushik, Optimum sizing of grid integrated hybrid PV-biomass energy system using an artificial bee colony algorithm. IET Renew. Power Gener. **10**(5) (2016)
4. E.B. Agyekum, C. Nutakor, Feasibility study and economic analysis of stand-alone hybrid energy system for southern Ghana. Sustain. Energy Technol. Assess. **39** (2020)
5. V. Boddapati, S.A. Daniel, Performance analysis and investigations of grid-connected solar power park in Kurnool, South India. Energy Sustain. Dev. **55**, 161–69 (2020). https://doi.org/10.1016/j.esd.2020.02.001
6. K.G. Jayanth, V. Boddapati, R.S. Geetha, Comparative study between three-leg and four-leg current-source inverter for solar PV application, in *International Conference on Power, Instrumentation, Control and Computing* (*PICC*) (Thrissur, 2018), pp. 1–6
7. M.A. Munjer, M.R.I. Sheikh, M.A. Alim, V. Boddapati, M.A. Musaib, Minimization of THD for MMC with triangular injection approach, in *International Conference on Electrical, Electronics, Computers, Communication, Mechanical and Computing* (*EECCMC-2018*) (Tamil Nadu, India, 2018)
8. M.A. Munjer, M.R.I. Sheikh, M.A. Alim, V. Boddapati, M.A. Musaib, Minimization of THD for multilevel converters with triangular injection approach, in *3rd International Conference for Convergence in Technology* (*I2CT*) (Pune, 2018), pp. 1–4
9. G. Rohani, M. Nour, Techno-economical analysis of stand-alone hybrid renewable power system for Ras Musherid in United Arab Emirates. Energy **64**, 828–841 (2014)
10. H.S. Das, A.H.M. Yatim, C.W. Tan, K. Yiew, Proposition of a PV/tidal power micro-hydro and diesel hybrid system: a Southeren Bangladesh focus. Renew. Sustain. Energy Rev. **53**, 1137–1148 (2016)